

Logarithmic of prime numbers to black hole entropy

M. Bousder^{1*}

¹LPHE-MS Laboratory, Department of physics,

Faculty of Science, Mohammed V University in Rabat, Rabat, Morocco

September 24, 2021

Abstract

In this paper, we study the thermofield double states of doubly-holographic gravity in two copies of the horizons. We show that the asymptotically AdS space-times describe an entangled states of a pair of CFTs based on the Farey sequence. We propose a new technique to geometrize the black hole horizon. Our protocol is based on the so-called Farey diagram. We construct states and entropies to describe the unit cells on the horizon. As a result, we have proved that the quantum states on the horizon are encoded by prime numbers. Therefore, we found that the entropy of the code space and area law are writtens in logarithmic form of the prime numbers. Our aim is to show that the number of connected components of the Farey sequence can build the Fermi–Dirac distribution. Finally, we mention the possibility to describe the quantum Hall effect by using the Farey diagram.

Keywords: Thermofield double, Black hole, ER=EPR, entanglement entropy.

1 Introduction

Recent work has focused on the issue of the thermofield double (TFD) states is a central ingredient. The connection between boundary information-theoretic quantities and bulk areas has been extended to a conjectured [1]. In parallel, there have also been numerous proposals to directly modeling the black hole (BH) evaporation and calculations of the entanglement entropy [2, 3]. The ER = EPR [4] has given a new perspective on the gauge/gravity correspondence. Under this paradigm, a pair of entangled black holes are joined by an Einstein-Rosen (ER) bridge. This suggests that there is a relation between quantum entanglement and geometric spatial. In [5], we are interested in the

*mostafa.bousder@um5.ac.ma

entanglement between the particles near the event horizon and antiparticle near the Cauchy horizon of EGB black hole. In [6] it was shown that the dual geometry is the usual eternal black hole. The entanglement entropy $S(A)$ of a boundary region is given by the area of RT surfaces, corresponding to the bulk minimal surface. The thread prescription which is equivalent to the quantum extremal surface (QES) prescription [7, 8]. In the Hayden-Preskill model [9], the information transfer from the black hole to the radiation. Let A be a boundary subregion of the bulk. The Ryu-Takayanagi formula $S(A) = \frac{1}{4G_N} \min_{\gamma: \partial\gamma=\partial A} \text{Area}(\gamma)$, relates the von Neumann entropy $S(A) = -Tr\rho \log \rho$ of the reduced density matrix ρ in holographic CFTs with the minimisation over the boundary subregion A . The entanglement entropy $S(A)$ of a boundary region is given by the area of RT surfaces γ , corresponding to the bulk minimal surface. The thread prescription which is equivalent to the quantum extremal surface (QES) prescription [10, 11]

$$S(A) = \min_{\gamma} \left[\frac{\text{Area}(\gamma)}{4G_N} + S_{\text{bulk}}(\sigma_{\gamma}) \right], \quad (1.1)$$

where σ_{γ} is the subregion of the bulk slice, which checked $\partial\sigma_{\gamma} = A \cup \gamma$ and $\gamma(AB) \neq \gamma(A) \cup \gamma(B)$. Let $\rho_{AB} \in L(H_{AB})$ be a state in the bipartite Hilbert space $H_{AB} = H_A \otimes H_B$. The entanglement of purification of ρ_{AB} is the mutual information $I(A, B) = S(A) + S(B) - S(A \cup B)$. A naive interpretation is that the bits encoding the microstate of A somehow “live on” the minimal surface Fig.1:

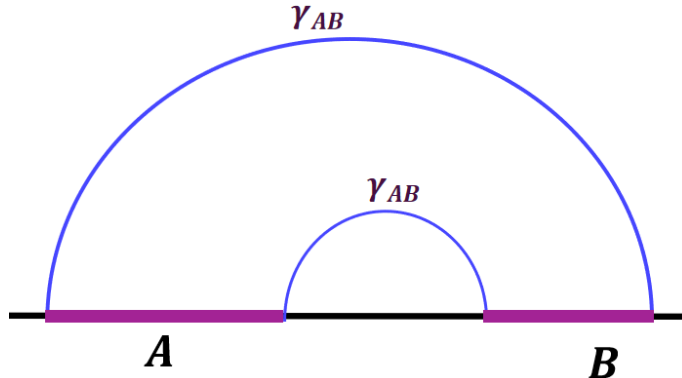


Figure 1: Two regions A and B are connected by the minimal bulk hypersurface $\gamma(AB)$.

Let $H = H_L \otimes H_R$ be the Hilbert space of the full CFT and $|u\rangle$ denote the quantum state of a system with N particles. Hamiltonian evolution is generated by $H_{TFD} = 1_L \otimes H_R + H_L \otimes 1_R$. Let us define the thermofield double state (TFD) as a particular

entangled state [12, 13]:

$$|TFD\rangle = \frac{1}{\sqrt{Z(\beta)}} \sum_j e^{-\beta E_j/2} |u_j\rangle_L \otimes |\bar{u}_j\rangle_R, \quad (1.2)$$

where Z is the partition function of the CFT at temperature $T = \beta^{-1}$ and $e^{-\beta E_j/2}/\sqrt{Z(\beta)}$ is a normalization factor such that $\langle TFD | TFD \rangle_k = 1$. The TFD state was suggested outside of the black holes. In this last equation, we consider t as a parameter labeling time-dependent TFD state at a common instant $|TFD(t)\rangle = e^{it(H_L+H_R)} |TFD\rangle$. In each of these states at time t , there exists a projection operator $P_t = |TFD(t)\rangle \langle TFD(t)|$. According to [4], two entangled states with different values of t are linked by the forward time evolution on the two sides of CFT . Note that the projection operator is expressed in terms of t . $|u_j\rangle_{LR}$ defined in the microscopic UV-complete theories, they create CFT states with energy [14]. By tracing out the exterior states in one horizon we obtain the density matrix. The mixed state given by the incoherent sum over all generalized TFD states $\rho_{TMD} = (1/N) \sum_j |TFD\rangle_j \langle TFD|$ call the the thermo-mixed double, where N the total number of basis states. The thermal density matrix as arising from entanglement. The corresponding bulk geometry of the wormhole is formed by $tr(\rho_{TMD}^2) = \sum_j e^{-2\beta E_j}/Z^2$, where $Z = \sum_j e^{-\beta E_j}$ is partition function, the square number 2 corresponds to the two horizons.

In this work, we present a preparation scheme for Farey sequence that can be implemented on a CFT_d on the boundary asymptotically AdS_{d+1} boundary of the dual gravity theory. Our first goal then is to figure out what the relation is between the TFD state the geometry of the region near horizon and. Our second goal is to determine the black hole statistic by using the TFD states. In this basis, we imagine a temperature at the horizon tends to ∞ . Then write the states $|TFD\rangle$ as a function of the states $|TFD(\beta = 0)\rangle$. This new technique will allow us to find another path to determine both the geometry, the state encoding and the statistics of the black hole. By studying the the number of BH states, we can understand that the BH undergoes the Fermi–Dirac particle-energy statistics.

2 Left and right horizons in CFT

We consider the TFD of dual to the left and right sides of the geometry by two copies of the horizons \mathcal{H}_L (left horizon) and \mathcal{H}_R (right horizon) in CFT. The eigenstate $|u_j\rangle_L$ (or $|\bar{u}_j\rangle_R$) of the CFT_L (or CFT_R) corresponding to the degrees of freedom in \mathcal{H}_L (or \mathcal{H}_R). In the context of holographic gravity, the two sides of CFT are connected by a wormhole, or ER bridge, according to the TFD states Eq.(1.2). The TFD is a maximally entangled state, which represents the formal purification of the thermal mixed state of

a one horizon (\mathcal{H}_L or \mathcal{H}_R) [15], with the reduced density matrix within *AdS/CFT* via the Ryu-Takayanagi formula [3]. We need to consider the TFD state describing the far region to describe the region outside the horizon. Let us define the vacuum state as a special case in which $|\psi\rangle = |TFD(\beta=0)\rangle_{LR} + |TFD(\beta=0)\rangle_{RL} \in H$. The meaning of $\beta=0$ is that the temperature is very high, and we assume that $\beta=0$ near the horizon. At this point, the entangled state can be decomposed into a *LR* and *RL* part as follows

$$|\psi\rangle = \frac{1}{\sqrt{Z(\beta)}} \left(\sum_{j=1}^{N_-} |u_j\rangle_L \otimes |\bar{u}_j\rangle_R + \sum_{k=1}^{N_+} |\bar{u}_k\rangle_R \otimes |u_k\rangle_L \right), \quad (2.1)$$

Here, N denotes the number of the quantum state, where $N = N_- + N_+$, with the number N_- and N_+ of copies of the states $|u\rangle$ and $|\bar{u}\rangle$, respectively, and $|u_j\rangle \neq |u_{j+1}\rangle$. We define an operator \mathcal{W} which verifies

$$\mathcal{W}|u_j\rangle_L = (-1)^{j-1}|u\rangle_L, \quad (2.2)$$

$$\mathcal{W}|\bar{u}_j\rangle_R = (-1)^{j-1}|\bar{u}\rangle_R, \quad (2.3)$$

$$\mathcal{W}^2 = 1, \quad (2.4)$$

or, equivalently,

$$\mathcal{W}|\psi\rangle \sim \sum_{j=1}^{N_-} (-1)^{j-1}|u\rangle|\bar{u}\rangle + \sum_{k=1}^{N_+} (-1)^{k-1}|\bar{u}\rangle|u\rangle, \quad (2.5)$$

which leads to

If N_- is even and N_+ is even, one obtain $\mathcal{W}|\psi\rangle = 0$.

If N_- is even and N_+ is odd, one get the pure state $\mathcal{W}|\psi\rangle \sim |\bar{u}\rangle|u\rangle$.

If N_- is odd and N_+ is even, one get the pure state $\mathcal{W}|\psi\rangle \sim |u\rangle|\bar{u}\rangle$.

If N_- is odd and N_+ is odd, one get the entangled state $\mathcal{W}|\psi\rangle \sim |u\rangle|\bar{u}\rangle + |\bar{u}\rangle|u\rangle$.

If N is infinite, one get the entangled state $\mathcal{W}|\psi\rangle_\infty \sim \frac{1}{2}(|u\rangle|\bar{u}\rangle + |\bar{u}\rangle|u\rangle)$, ($\zeta(0) = 1/2$, the analytic continuation of the Riemann zeta function).

We can map initial state $|\bar{u}\rangle|u\rangle$ and final state $|u\rangle|\bar{u}\rangle$ in the CFT, then we can compute the entanglement between the two states in the CFT. This procedure can represent by the following quantification. The states $|0\rangle$ and $|\bar{0}\rangle$ are the Rindler vacuum states in the two exterior region horizons in the right and left horizons, respectively. The state $|0\rangle|\bar{0}\rangle$ is the outside horizons vacuum states. The state $\mathcal{W}|\psi\rangle$ is transformed to

$$\mathcal{W}|\psi\rangle \sim \alpha|u\rangle|\bar{u}\rangle + \beta|\bar{u}\rangle|u\rangle, \quad (2.6)$$

with

$$(\alpha, \beta) = \begin{cases} (0, 0) \\ (0, 1) \\ (1, 0) \\ (1/2, 1/2) \\ (1, 1) \end{cases}, \quad (2.7)$$

such that $(\alpha, \beta) \geq (0, 0)$ are quantum numbers. The results of this section suggest that $|TFD\rangle = \mathcal{W}\left(\sum_j \sqrt{p_j} e^{i\omega_j} |\psi\rangle_j\right)$. We can reexpress the TFD states in terms of the ($\beta = 0$) modes as

$$|TFD\rangle = \frac{1}{\sqrt{Z(\beta)}} \sum_{j=1}^N e^{-\beta E_j/2} \mathcal{W}\left(|TFD_j(\beta=0)\rangle_{LR} + |TFD_j(\beta=0)\rangle_{RL}\right). \quad (2.8)$$

As previously mentioned, we adopt the states $|TFD(\beta=0)\rangle$ to evaluate the geometric approach of two copies of the horizons in the holographic CFT. The volume of this geometry increases in time according to the number of degrees of freedom of the boundary theory. Note that we can rewrite the state $|\psi\rangle$ as

$$|\psi\rangle \sim N_+ |u\rangle |\bar{u}\rangle + N_- |\bar{u}\rangle |u\rangle. \quad (2.9)$$

For entangled states, the left and right systems are identical ($N_- = N_+ = N/2$), the state $|\psi\rangle$ can be represented as $|\psi\rangle \sim \frac{N}{2} (|u\rangle |\bar{u}\rangle + |\bar{u}\rangle |u\rangle)$. Comparing Eq.(2.1) to Eq.(2.6), we conclude that

$$|u\bar{u}\rangle = \frac{N_- - \beta}{\alpha - N_+} |\bar{u}u\rangle. \quad (2.10)$$

Using the normalization: $\langle u\bar{u} | u\bar{u} \rangle = 1$, we notice that $\alpha + \beta = N$ or $\alpha - \beta = N_+ - N_-$. Then, by applying this observation, we obtain

$$\begin{aligned} |u\bar{u}\rangle &= +|\bar{u}u\rangle \text{ for } \alpha + \beta = N, \\ |u\bar{u}\rangle &= -|\bar{u}u\rangle \text{ for } \alpha - \beta = N_+ - N_-. \end{aligned} \quad (2.11)$$

Since the Eq.(2.7) satisfy $\alpha + \beta = \{0, 1, 2\}$ and $\alpha - \beta = \{-1, 0, 1\}$, we can reexpress the generator in terms of the N modes as

$$\begin{aligned} |u\bar{u}\rangle &= +|\bar{u}u\rangle \text{ for } N = \{1, 2\}, \\ |u\bar{u}\rangle &= -|\bar{u}u\rangle \text{ for } N \geq 2. \end{aligned} \quad (2.12)$$

These two relationships above, implies that the state $\mathcal{W}|\psi\rangle$ is not an entangled state

$$|\psi\rangle \xrightarrow{\text{entanglement removal}} \mathcal{W}|\psi\rangle. \quad (2.13)$$

To describe the Majorana states, one could also choose $N = 2$ for the first case. For us, the change of sign (+) to (−) in $N = 2$, lead to additional degeneracy.

Now, we consider $N_+ = N_- = N/2$. The coherent states can be expressed in terms of Fock states in the standard way as

$$|\psi\rangle = \frac{1}{\sqrt{Z(\beta)}} \left[\sum_{j=1}^{N_-} e^{-\beta E_j/2} |u_j\rangle_L \otimes e^{+\beta E_j/2} |\bar{u}_j\rangle_R + \sum_{k=1}^{N_+} e^{+\beta E_k/2} |\bar{u}_k\rangle_R \otimes e^{-\beta E_k/2} |u_k\rangle_L \right]. \quad (2.14)$$

We use the transformation

$$\sqrt{2}e^{+\beta E_j/2} |\bar{u}_j\rangle_R \longrightarrow |\bar{u}_j^*\rangle_R, \quad (2.15)$$

then, the evolution of the horizon is then described by the following entangled state

$$|\psi(t)\rangle = \frac{1}{\sqrt{2}} (|TFD^*(t)\rangle_{LR} + |TFD^*(t)\rangle_{RL}), \quad (2.16)$$

where $|TFD^*(t)\rangle_{LR}$ is the evolution of the TFD state in the horizon from L to R at time t .

3 Farey diagram of the horizon geometry

We now discuss how the near horizon geometry is described from the point of view of the Farey diagram. As illustrated above, we also wish to express the state $|u\bar{u}\rangle$ in terms of the number of states acting on the state $|\bar{u}u\rangle$. Let us start by considering the three cases $(\alpha, \beta) = \{(0, 0); (0, 1); (1, 0)\}$ Eqs.(2.6,2.9). Then, the corresponding states generated by

$$|u\bar{u}\rangle_{\beta=0} = \frac{N_-}{\alpha - N_+} |\bar{u}u\rangle, \quad |u\bar{u}\rangle_{\alpha=0} = \frac{\beta - N_-}{N_+} |\bar{u}u\rangle. \quad (3.1)$$

A new value of α and β is in principle determined by the normalization: $\langle u\bar{u} | u\bar{u} \rangle = 1$, one could take

$$\alpha = \{(N_+ - N_-); N\}_{\beta=0}, \quad \beta = \{(N_- - N_+); N\}_{\alpha=0}. \quad (3.2)$$

Here, we have $N \neq 0$. To check the conditions Eqs.(2.7,3.2), we distinguish between two cases:

(i) For the two cases: $\alpha = N_+ - N_-$ or $\beta = N_- - N_+$, the number of states are $N > 1$. (ii) For $\alpha = N$ or $\beta = N$, we have obtained only $\alpha = \beta = N = 1$, i.e. only one state in the system. When $N = N_+ - N_-$, one could take one degenerate solution corresponding to $N_- = 0$, which agrees with the violation of CP symmetry between matter and antimatter [16]. Therefore, the black hole behaves under the normalizable states as Schwarzschild

or extremal black hole. Obviously, this distinction between the cases of α and β , can simplify the equation Eq.(3.1) as

$$\begin{aligned} |u\bar{u}\rangle &= |\bar{u}u\rangle \text{ for } N = 1, \\ |u\bar{u}\rangle &= -|\bar{u}u\rangle \text{ for } N > 1. \end{aligned} \quad (3.3)$$

Then, the corresponding states generated by

$$|u\bar{u}\rangle = (-1)^{1+\delta_N} |\bar{u}u\rangle, \quad (3.4)$$

where $\delta_N (N = 1) = 1$ and $\delta_N (N > 1) = 0$. Both cases Eq.(3.1) give the same result above. These states are invariant under the transformation $\delta_N \rightarrow -\delta_N$. Therefore, the state $|u\bar{u}\rangle$ is formulated in terms of the state $|\bar{u}u\rangle$, the main reason is that this relation gives an aspect in of a wormhole between the two states. It was explicitly confirmed by ER bridges from ER = EPR [17]. This result is equivalent to the sum of the Möbius function $\mu(N)$ over N

$$\delta_N = \sum_{k|N} \mu(k) = \begin{cases} 1 & \text{if } N = 1 \\ 0 & \text{if } N > 1 \end{cases}, \quad (3.5)$$

where

$$\mu(N) = \sum_{\substack{1 \leq k \leq N \\ \gcd(k, N)=1}} e^{2\pi i \frac{k}{N}}. \quad (3.6)$$

This algebraic proof shows that the connection between the two horizons \mathcal{H}_L and \mathcal{H}_R is realised the Möbius function. Thus allowing to the Mertens function:

$$\mathcal{M}_N = \sum_{k=1}^N \mu(k) = -1 + \sum_{n \in \mathcal{F}_N} e^{2\pi i n}, \quad (3.7)$$

where \mathcal{F}_N denotes the Farey sequence of order N [18]. The quantum number α Eq.(2.7), consists of a contribution from the Farey sequence. The number α can be encoded into $\mathcal{F}_2 = \left\{ \frac{0}{1}, \frac{1}{2}, \frac{1}{1} \right\}$. Let us consider the fraction $\frac{a}{b} \in \mathcal{F}_N$, there is a Ford circle $\mathcal{C} \left[\frac{a}{b} \right]$ with the radius $1/(2b^2)$ and centre at $(\frac{a}{b}, \frac{1}{2b^2})$. The Farey diagram describes a geometry near the AdS horizon. The Farey diagram \mathcal{F}_N of order $N \rightarrow \infty$ is given by

$$\mathcal{F}_\infty = \left\{ \frac{a}{b} : (a, b) \in \mathbb{Z}, \gcd(a, b) = 1 \right\} \cup \left\{ \frac{1}{0} \right\}. \quad (3.8)$$

The graph \mathcal{F}_N is associate to a closed surface of genus. This represents that the edges indicate geometric intersection number equal to N [19]. In fact, we hcan also study the possible symmetries of the Farey diagram using 2×2 matrices correspond to linear transformations of the plane from linear algebra, see Fig.2.

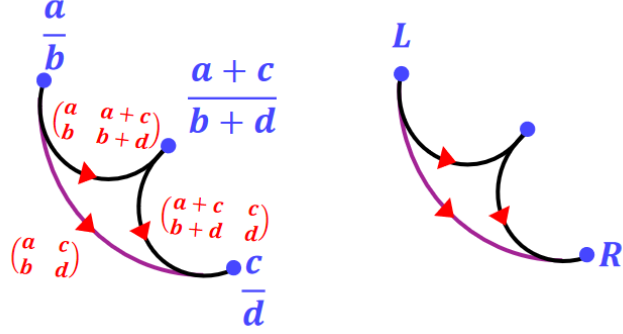


Figure 2: To go from \mathcal{H}_L to \mathcal{H}_R , we can use the 2×2 matrices correspond to linear transformations, which are formed by Farey sequence.

Each such vertices of $\frac{a}{b} \in \mathcal{F}_N$ has two primitive elements (a, b) and $(-a, -b)$. This makes it possible that a/b and $(-a) / (-b)$ are two different descriptions of the same state. In Fig.3 we give an example of Farey diagram.

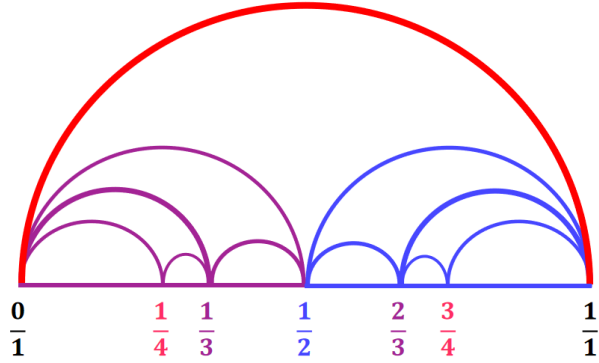


Figure 3: The Farey diagram \mathcal{F}_4 represented with circular arcs by the fraction values.

Each curve in Fig.4, represents a geodesic connection entanglement wedge between two horizon points.

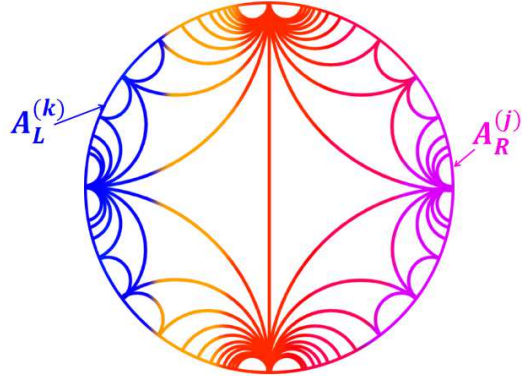


Figure 4: The bulk minimal surfaces of the subregions \mathcal{A}_L and \mathcal{A}_R .

The Farey sequences of order n in $CFT = \mathcal{A}_L \cup \mathcal{A}_R$ circle encode an information contained in a set of coefficients $\frac{a}{b}$. This result can be extended to include subregions Fig.4: $\mathcal{A}_{L \text{ or } R}^{(n)} \subset \mathcal{A}_{L \text{ or } R}^{(n-1)} \subset \cdots \subset \mathcal{A}_{L \text{ or } R}^{(1)} \subset \mathcal{A}_{L \text{ or } R}$. Following this procedure we obtained the n -point correlation function corresponding to the fraction points of the Farey diagram. Later, we will see a new description of n -point correlation function, like q cell is characterized by q -bit code.

4 Unitary prime describtion of the horizon

The Farey diagram of the near horizon geometry is a construction of multi-boundary connection between microstates. The Multi-boundary can be obtained by evaluating the Euclidean CFT path integral on a cut Riemann surface [20]. The connection between the circles in the Farey diagram, represent the encoding of information. The number of connected components of \mathcal{F}_N is constructed as follows

$$N_{con}(\mathcal{F}_N) = \begin{cases} p^{q-1}(p+1) & \text{if } N = p^q \\ \infty & \text{otherwise.} \end{cases}, \quad (4.1)$$

where p is a prime and q is a positive integer. When N is not a prime power, the number of connected components is infinite. We are interested by the solution where $N = p^q$. This indicates that the convergence to the large N limit is fast. The exponential degeneracy of the field theory vacuum states, indicated by the number

$$N_{vac} = e^{q \log p}, \quad (4.2)$$

which corresponds to the number of vacuum states in [21] if the entropy of a vacuum is $S_{vac} = ql_P^2 \log p$, where $l_P = \sqrt{\hbar G/c^3}$ is the Planck length. Therefore, the logarithm of the prime number of independent quantum states describes the boundary structure of the black hole. This number is also equivalent to the number of black hole states consistent with the boundary structure described above. We consider a lattice system in the horizon, each q cell is describe by a Farey fraction $\frac{a}{b}$. This implies that S_{vac} is obtained only after we include a prime number p . Also N_{vac} represents the number of possible independent ways to describe CFT on a fixed classical spacetime background (semi-classical physics). Let us elaborate the entropy of the near horizon region in a similar way to the Bekenstein-Hawking formula. The black hole first law of thermodynamics reads $S_{BH} = \int dM/T$. The validity of the generalized second law of thermodynamics suggests that it is given by the exponential of the Bekenstein-Hawking entropy $S_{BH} = A/4$ [21], where A is the area of the horizon. More precisely, the black hole horizon is encoded on each q cell by the prime number of states

$$p = \exp(A/4ql_P^2). \quad (4.3)$$

According to [21], the term $\exp(A/4ql_P^2)$ is the total number of black hole vacuum states $|\psi_q\rangle$ for a fixed mass, where $q = 1, 2, \dots, p$. The entropy S_{BH} will be the encoding of p for p cell and we write that

$$S_{BH} = pl_P^2 \log p. \quad (4.4)$$

Therefore, the prime numbers p are always the total number of states of a black hole. In this view, the state $|u\bar{u}\rangle$ gives the unit cell with area l_P^2 . Sometimes the existence of the connected components of \mathcal{F}_N Eq.(4.1) is presented as a consequence of the area law. This shows that \mathcal{F}_N diagram is a new geometrization of black hole.

5 Fermi–Dirac of prime number state

Next we build a unitary processes, describing the interior and near horizon the black hole vacuum states. The number of excited states that can be built is

$$N_{tot} = N_{con} = \left(1 + \frac{1}{p}\right) \times N_{vac}, \quad (5.1)$$

when $p = \infty$ we get $N_{tot} = N_{vac}$. The prime number p represents the encoding of the information on the horizon. As a result, we find the Fermi–Dirac particle-energy distribution

$$N_{vac} = \frac{N_{tot}}{e^{-\frac{S_{BH}}{ql_P^2}} + 1}. \quad (5.2)$$

If $q = 0$, we obtain $N_{vac} = N_{tot}$. We can immediately see that the simplest horizon corresponds to a thermal ensemble of Fermi–Dirac configuration, which justifies our focus on the number of connected components of \mathcal{F}_N . Therefore, the prime power N obtained by the Farey sequence, generates the Fermi–Dirac statistics. This implies that we can interpret $S_q = ql_P^2$ as an entropy of q cell of the horizon with the quantum microstates $|\psi_q\rangle$, where $q = 1, 2, \dots, p$ and p is the total number of black hole states.

The horizon and near horizon region are described by the microstate $|\psi_q\rangle$. The analysis described above indicates that the vacuum state is defined by $a^{(1)}|\psi_1\rangle = 0$ and $a^{(q)}|\psi_q\rangle = |\psi_{q-1}\rangle$, where $a^{(1)}$ is annihilates all the vacuum states. A state in which describes the black hole can be constructed by acting $a^{(q-1)\dagger}|\psi_{q-1}\rangle = |\psi_q\rangle$, where $a^{(q)\dagger}/a^{(q)}$ are the creation/annihilation operators of order q . For $p = 2$ we obtain $N_{vac} = 2^q$. The states $|\psi_{r>n}\rangle$ corresponding to the black hole radiation by thermal ensembles of excitations with the temperatures $1/\beta$. Later, we shall see that the quantum Hall effect from this entropy. Using Eq.(5.2), we define the entropy of the code space $H_{code} \subseteq H_{CFT}$ [22] of q cell in the horizon by

$$S_q = l_P^2 \frac{\log N_{vac}}{\log p}. \quad (5.3)$$

According to [22], we notice that $S_p \sim \log |H_{code}|$. In this case there exists a subspace $H_{code}^{(q)} \subseteq H_{code}$ of q cell (q microstates). By equivalence, we get $S_q \sim \log |H_{code}^{(q)}|$. The q cell is characterized by q -bit code [23]. So that $\log |N_{vac}|^{\frac{l_P^2}{\log p}} = \log |H_{code}^{(q)}|$. We can express the Bekenstein-Hawking entropy and the entropy of a vacuum of coding entropy in terms of the encoding entropy S_q as $S_{vac} = S_q \log p$ and $S_{BH} = S_p \log p$. The presence of $\log p$ in the entropy S_{BH} , implies a discontinuity of the entropy at the level of the information coding.

6 Quantum Hall effect in the horizon

Using the black hole first law of thermodynamics for semiclassical black holes reads $S_{BH} = \int dM/T = A/4$. One could also choose $S_p \equiv \int dM/T_p$. In the simple case, we define the resistance R_H which depends on the temperature of p cell as

$$R_H(q) = \frac{4\pi\varepsilon_0 k_B T_p \log p}{c^3 M} \equiv \frac{T_p \log p}{M}, \quad (6.1)$$

or equivalently

$$R_H(p) = \frac{1}{l_P^2 p}. \quad (6.2)$$

We notice that the expression Eq.(6.2) is exactly like with the Hall resistance R_H in the quantum Hall effect, because p is integer: $R_H = h/e^2\nu = 1/G_H$, where h is Planck's constante, e is the elementary charge and G_H is the quantized Hall conductivity. The number ν can take on either integer ($\nu = 1, 2, 3, \dots$) or fractional $\nu = (1/3, 2/5, 3/7, \dots)$. It is a simple consequence of the motion of charged particles in the near horizon region. In this case the entropy Eq.(5.3) represent the quantized Hall conductivity [24], i.e. l_P is the elementary area of the elementary charge e . The most important remark is when the number of p cells is infinite, the resistance R_H is zero, then there is no more evaporation of the black hole ($T_\infty = 0$).

From Eqs.(5.3,6.1,6.2) we get

$$S_p \equiv G_H \propto \frac{1}{T_p}. \quad (6.3)$$

This last relation is similar to **Wiedemann-Franz law** [25], i.e. the electrical conductivity of metals at normal temperatures is inversely proportional to the temperature. Also we have $R_H(p) = 1/S_{BH} \sim 1/A$, which checks the law of the **Pouillet's law** [26]. Recall that the quantum Hall is observed in two-dimensional electron systems. This result corresponds exactly with area law, which connects the entropy of black hole with the surface of horizon. We notice that the relation between area law and the entropy S_q ,

is described by the relation Eq.(5.2). The electrical resistance in the Pouillet's law can be expressed as

$$R_H = \frac{r}{A\sigma}, \quad (6.4)$$

where A is the cross-sectional area, r is a distance between the horizon and the charged near horizon region, σ is the conductivity of the matter (material) in the near horizon region. From Eqs.(6.2,6.4), we obtain

$$A\sigma = prl_P^2. \quad (6.5)$$

If the total number of cells equal to 1; i.e. $n = A/4l_P^2 = 1$, we find $\sigma_1 = \frac{r}{4}$. If we assume that r is the thickness of the region between the black hole and the photon sphere, we can express in this case σ as $\sigma_1 = \frac{1}{4}(r_{ps} - r_H)$, where r_{ps} is the radius of the photon sphere. In this region, we have electrically charged particle interacting with electromagnetic field. Then, we propose a representation of the near horizon geometry in terms of magnetic field B . We have a creation of a magnetic field on each cell with the magnetic length l_B , which will be proportional to Planck length l_P . We can interpret this result by creating of an electric current passing through the horizon in a magnetic field.

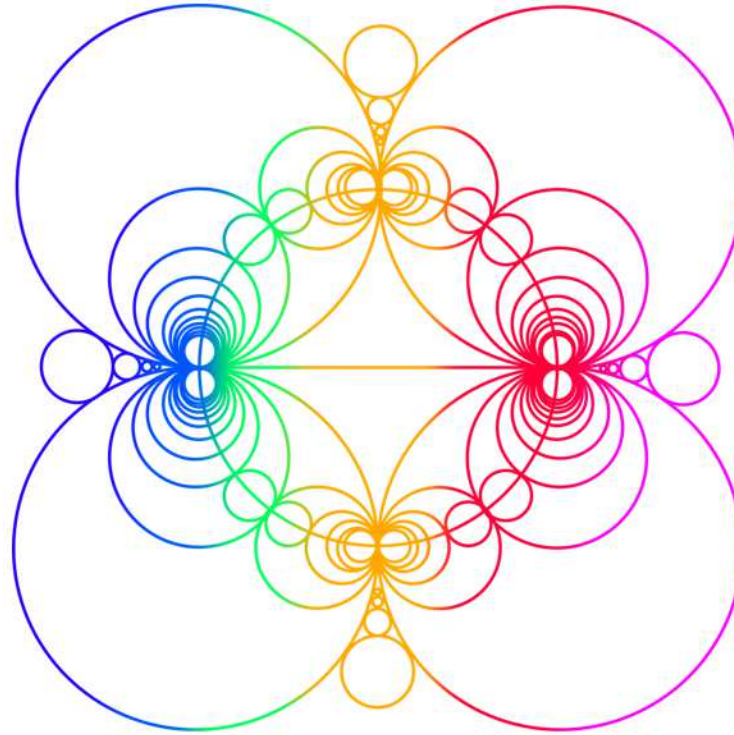


Figure 5: To obtain Farey diagram, we employ the Ford circle. The diagram also makes it very clear that there the event horizons in Ford space. The Ford circle are equivalent to the cyclotron orbit of the edge states.

Comparing Fig.5 to Fig.3 to the constructing wormhole spatial geometries, we can use the quotients of the Poincaré disk [27]. From Farey graph Fig.5, we notice that the circles are only the displacement of charges on the black hole surface, and the interior of the black hole behaves as a topological insulator. In a classical point of view, the charged particles move in circular motion (the cyclotron orbit) in the horizon with a uniform perpendicular magnetic field. This rotational motion predicts the existence of edge states in the the black hole horizon. This concept makes it possible to see the lines are equipotential lines.

This paper, based on the geometrization of the near-horizon region. We noticed that there is a new geometry hiding in the TFD states. In this framework we have defined and studied new states expressed as a function of TFD state and for an infinite temperature. We have divided the horizon into two sub-regions; the left horizon \mathcal{H}_L and the right horizon \mathcal{H}_R . Our results clearly demonstrate that the connection between the two horizons \mathcal{H}_L and \mathcal{H}_R is realised by the Möbius function. The evolution of the TFD state in the horizon allows to distinguish between two cases of the number of particles $\{N = 1, N \succ 1\}$. We have geometrized the near horizon region by the Farey diagram \mathcal{F}_N . The use of the number of connected components of \mathcal{F}_N , leads to a find a unitary describtion of the horizon. This description is done by the Fermi–Dirac distribution.

From this distribution, we have demonstrate the existence of cells that contain quantum information. The number of connected components in Farey diagram encode the quantum information in cells. The q cell is characterized by q -bit code and the prime number of states p . Each q cell is described by the entropy $S_q = ql_P^2$ and the quantum microstates $|\psi_q\rangle$. If q equals the total number p (prime number) of cells on the horizon, the Bekenstein-Hawking entropy will be equal to $pl_P^2 \log p$. Following this procedure, we have write the Bekenstein-Hawking entropy in logarithmic term. We have found the expression of the horizon resistance in terms of $1/p$ and which is exactly similar to the Hall resistance R_H in the quantum Hall effect. The formulation of this resistance leads to a new description of the black hole evaporation. As a brief summary, we has used the relationship between geometry and numbers to describe the encoding of quantum information on the horizon, which shows us that the black hole behaves like a topological insulator. The geometry behind TFD states near horizon, is represented by the Farey diagram, behind this diagram it has a physics description, this is a unitary describtion of quantum Hall effect in the Fermi–Dirac statistics.

References

- [1] Bao, N., Chatwin-Davies, A., Pollack, J., & Remmen, G. N. (2019). *Towards a bit threads derivation of holographic entanglement of purification*. *J. High Energy Phys*, 2019(7), 1-24.
- [2] Akal, I., Kusuki, Y., Shiba, N., Takayanagi, T., & Wei, Z. (2021). *Entanglement Entropy in a Holographic Moving Mirror and the Page Curve*, *Phys. Rev. Lett.*, 126(6), 061604.
- [3] Ryu, S., & Takayanagi, T. (2006), *Holographic derivation of entanglement entropy from the anti-de sitter space/conformal field theory correspondence*, *Phys. Rev. Lett.*, 96(18), 181602.
- [4] Maldacena, J., & Susskind, L. (2013). *Cool horizons for entangled black holes*, *Fortschritte der Phys.*, 61(9), 781-811.
- [5] Bousder, M., & Bennai, M. (2021), *Particle-antiparticle in 4D charged Einstein-Gauss-Bonnet black hole*. *Phys. Lett. B*, 817, 136343.
- [6] Freyr, G. F., Lukas, S., Watse, S., & Lárus, T. (2020). *Page curve for an evaporating black hole*. *J. High Energy Phys.*, 2020(5).

- [7] Cottrell, W., Freivogel, B., Hofman, D. M., & Lokhande, S. F. (2019). *How to build the thermofield double state*. *J. High Energy Phys.*, 2019(2), 58.
- [8] Freedman, M., & Headrick, M. (2017). *Bit threads and holographic entanglement*. *Commun. Math. Phys.*, 352(1), 407-438.
- [9] Hayden, P., & Preskill, J. (2007). *Black holes as mirrors: quantum information in random subsystems*. *J. High Energy Phys.*, 2007(09), 120.
- [10] Freedman, M., & Headrick, M. (2017). *Bit threads and holographic entanglement*. *Communications in Mathematical Physics*, 352(1), 407-438.
- [11] Guo, G., Wang, P., Wu, H., & Yang, H. (2021). *Scalarized Einstein-Maxwell-scalar Black Holes in Anti-de Sitter Spacetime*. *arXiv preprint arXiv: 2102.04015*.
- [12] Remmen, G. N., Bao, N., & Pollack, J. (2016), *Entanglement conservation, ER=EPR, and a new classical area theorem for wormholes*, *J. High Energy Phys.*, 2016(7), 1-15.
- [13] Dai, D. C., Minic, D., Stojkovic, D., & Fu, C. (2020), *Testing the ER= EPR conjecture*, *Phys. Rev. D*, 102(6), 066004.
- [14] Maldacena, J. (2003). *Eternal black holes in anti-de Sitter*. *J. High Energy Phys.*, 2003(04), 021.
- [15] Verlinde, H. (2020), *ER= EPR revisited: on the entropy of an Einstein-Rosen bridge*, *arXiv preprint arXiv: 2003.13117*.
- [16] Pascoli, Silvia, and Jessica Turner (2020), *Matter–antimatter symmetry violated*, *Nature*, 323-324.
- [17] Gharibyan, H., & Penna, R. F. (2014), *Are entangled particles connected by wormholes? Evidence for the ER= EPR conjecture from entropy inequalities*, *Phys. Rev. D*, 89(6), 066001.
- [18] Mukherjee, A., Mukhi, S., & Nigam, R. (2007). *Dyon death eaters*. *J. High Energy Phys.*, 2007(10), 037.
- [19] Gaster, J., Lopez, M., Rexer, E., Riell, Z., & Xiao, Y. (2020). *Combinatorics of \$k\\$-Farey graphs*. *Rocky Mt J Math*, 50(1), 135-151.
- [20] Krasnov, K. (2000). *Holography and Riemann surfaces*. *arXiv preprint hep-th/0005106*.

- [21] Nomura, Y., & Weinberg, S. J. (2014). *Entropy of a vacuum: What does the covariant entropy count?*. *Phys. Rev. D*, 90(10), 104003.
- [22] Penington, G. (2020), *Entanglement wedge reconstruction and the information paradox*, *J. High Energy Phys.*, 2020(9), 1-84.
- [23] Hayden, P., & Penington, G. (2020). *Approximate quantum error correction revisited: introducing the alpha-bit*. *Commun. Math. Phys.*, 374(2), 369-432.
- [24] Hasan, M. Z., & Kane, C. L. (2010). *Colloquium: topological insulators*. *Rev. Mod. Phys.*, 82(4), 3045.
- [25] Kubala, B., König, J., & Pekola, J. (2008). *Violation of the Wiedemann-Franz law in a single-electron transistor*. *Phys. Rev. Lett.*, 100(6), 066801.
- [26] Zyulkov, I., Armini, S., Opsomer, K., Detavernier, C., & De Gendt, S. (2019). *Selective electroless deposition of cobalt using amino-terminated SAMs*. *J. Mater. Chem. C*, 7(15), 4392-4402.
- [27] Akers, C., Engelhardt, N., & Harlow, D. (2020). *Simple holographic models of black hole evaporation*. *J. High Energy Phys.*, 2020(8), 1-14.